

Research Article

Study on Presplitting Blasting the Roof Strata of Adjacent Roadway to Control Roadway Deformation

Xiaojie Yang,^{1,2} Chaowen Hu ,^{1,2} Manchao He,¹ Haohao Wang,¹ Yubo Zhou ,²
Xiaoyu Liu,^{1,2} Enze Zhen,^{1,2} and Xingen Ma^{1,2}

¹State Key Laboratory for GeoMechanics and Deep Underground Engineering, China University of Mining and Technology, Beijing 100083, China

²School of Mechanic and Civil Engineering, China University of Mining and Technology, Beijing 100083, China

Correspondence should be addressed to Chaowen Hu; 916167981@qq.com

Xiaojie Yang and Chaowen Hu contributed equally to this work.

Received 24 August 2018; Revised 21 October 2018; Accepted 13 November 2018; Published 16 January 2019

Academic Editor: Salvatore Russo

Copyright © 2019 Xiaojie Yang et al. This is an open access article distributed under the Creative Commons Attribution License, which permits unrestricted use, distribution, and reproduction in any medium, provided the original work is properly cited.

In order to solve the problem of roadway deformation based on the theory of “short cantilever beam by roof cutting,” the method of “pressure relief by roof cutting in the adjacent roadway” is proposed. Through presplitting blasting the roadway hard rock layer, the stress propagation path is cut off, and the surrounding rock stress environment of the roadway is improved, to achieve the purpose of controlling the deformation of the roadway caused by stress. Through theoretical analysis, it is determined that the depth of the presplitting blasthole is 17 m, and the angle with the vertical direction is 10°. Based on in situ measurements and tests, by presplitting blasting the roof strata of the adjacent roadway, the maximal value of the working resistance of the hydraulic support in the presplitting blasting side of the working face decreased by 24.9%, and the average volumes of the maximum floor heave, the maximum roof subsidence, and the maximum ribs displacement were reduced by 50.1%, 34.9%, and 41.7%, respectively. This method completely changes the traditional thought patterns of “reinforcing support” to control roadway deformation from “strong support” to “pressure relief.” It provides a new idea for controlling the roadway deformation.

1. Introduction

A protective coal pillar of 10~30 m should be left between adjacent working faces to prevent the roadway from deformation and damage in traditional long wall mining [1–3]. As the depth of mining continues to increase, the surrounding rock of the roadway gradually exhibits the characteristics of soft rock under the influence of high ground stress, high ground temperature, high osmotic pressure, and strong mining disturbance [4–7]. The velocity and time of creep are greater than those of shallow rock strata [8, 9]. The roadway deformation increases significantly during mining, and the floor heave is especially severe. The roadway deformation not only affects pedestrians, transportation, and ventilation but also causes the entire roadway to be scrapped in serious cases, which seriously affects the safety of mining. The roof and ribs of roadways in China are usually supported by “bolt/cable + mesh,” while the

floor is usually unsupported. Although the protective coal pillar is left, the floor heave is still the most serious problem in roadway deformation. At present, generally, the methods of undercutting the floor, reinforcement, or pressure relief are used to control the floor heave [10–12].

In 2008, the “short cantilever beam by roof cutting” theory [13–16] was put forward by Professor Manchao He, an academician of the Chinese Academy of Sciences. In this theory, the ground pressure is used for the purpose of advancing the roof caving by precutting to form a cantilever beam above the gob-side gateway. When the precutting is performed on the roof of the gateway, the transmission of overburden pressure is cut off, which mitigates the ground pressure on the roadway. Also, part of the roof rock mass is driven down and fills the gob in time to support the overlying rock strata, reduce the suspension area, and reduce the influence on the roadway.

Based on this theory, this study proposes the method of “pressure relief by roof cutting in the adjacent roadway” to control roadway deformation. The purposes of presplitting blasting the roof strata of the adjacent roadway are to cut off the stress propagation path and to improve the surrounding rock stress conditions of the roadway to control the roadway deformation [17–20]. As shown in Figure 1, rock B and rock C are the main roof above the gob of the adjacent roadway, which is driven by overburden pressure. Rock A is the main roof above the coal pillar and roadway. When the adjacent working face is mined, since part of the roof strata of the adjacent roadway has been cut off, rock A is completely separated from rock B, which mitigates the influence of rock B and rock C on the roadway when they collapse, and the transmission of overburden pressure is cut off. This achieves the purpose of reducing the deformation of the surrounding rock and protecting the roadway.

This study chose the 72909 ventilation roadway of the Du’erping coal mine in Shanxi Province in China as the engineering background to verify the effect of roadway deformation control by presplitting blasting the roof strata of the adjacent roadway. As shown in Figure 2(a), the Du’erping coal mine (Xishan Coal Electricity Group Co., Ltd.) is in Taiyuan city in China’s Shanxi Province, and the location of the 72909 ventilation roadway is shown in Figure 2(b).

2. Influenced Factors of Roadway Deformation

Ground stresses, the strength of the surrounding rock, and the support of the roadway are the most important factors that affect the stability of the roadway surrounding rock [21–24]. The roof and ribs of the roadways in China are usually supported by “bolt/cable + mesh,” while the floor is usually unsupported, and the floor heave is common; therefore, this research focused on the influence of ground stress and floor lithology on the floor heave. According to references [25, 26], the rising and compressing coal rock layers are distributed from the floor to the deep, and the dividing point of the rising and compressing coal rock layers is the zero-displacement point; the tensile strain and compressive strain coal strata are distributed from the floor to the deep, and the dividing point of the tensile strain and compressive strain coal stratum is the zero-strain point. With the zero-displacement point and zero-strain point as the boundary, the floor strata are divided into tensile strain rise zone, tensile strain compression zone, and compressive strain compression zone. Figure 3(a) demonstrates the influence of floor lithology on the floor heave when the other factors are fixed. The mechanical parameters of floor lithology are shown in Table 1. (1) As the floor strength decreases, the zero-displacement point and zero-strain point develop toward the depth of the floor. (2) When the floor is hard or medium-hard rock, as the floor lithology changes, the changes in the zero-displacement point and the zero-strain point are small, and the variation ranges are 0.30–0.57 m and 2.57–2.80 m, respectively. (3) When the floor is soft or extremely soft rock, as the floor lithology changes, the

zero-displacement point and zero-strain point are transferred quickly and deeply into the floor, the zero-displacement point changes from 1.10 m to 2.95 m, and the zero-strain point changes from 3.13 m to 5.67 m. Figure 3(b) demonstrates the influence of horizontal stress on the floor heave when the other factors are fixed. (1) The critical point of the coefficient of horizontal pressure is 1.8 when the coefficient of horizontal pressure is less than 1.8, and the change in the zero-strain point is small. Otherwise, the zero-strain point increases significantly. (2) With the increase in horizontal stress, the zero-displacement point has basically a linear increase.

As shown in Figure 3, the rock strength of the surrounding rock and the magnitude of ground stress all have a great influence on the surrounding rock deformation of the roadway. At present, the methods of reinforced support or grouting in the surrounding rock are based on increasing the strength of the surrounding rock. However, the control effect of the surrounding rock deformation is poor, particularly in a roadway with high ground stress. So, this study proposes the method of presplitting blasting the roof strata of the adjacent roadway to control roadway deformation. The purpose of controlling the surrounding rock deformation is achieved by roof cutting to relieve the mining pressure.

3. Engineering Background

3.1. General Situation of the Working Face. The 72909 working face is located in panel South-9, the primary mineable coal bed is the #2 coal seam, the mining depth of the #2 coal seam is 505–647 m, the average thickness is 2.93 m, and the dip angle is 6°. The strike length and the working face length of 72909 are 1595 m and 216 m, respectively. The surrounding rock of the 72909 ventilation roadway is mainly composed of mudstone and sandstone, and the detailed strata histogram is shown in Figure 4.

3.2. Geomechanical Test of Roadway Surrounding Rock

3.2.1. Layout of Measure Points. In order to obtain an overall understanding of the geological mechanics of the surrounding rock of the #2 coal seam, a total of three measuring points was arranged on the site. To ensure whether the test was accurate and representative, the selection of the measuring points followed the principles: (1) large tectonic zones were avoided; (2) the rock strata for the test was relatively intact; (3) measuring points maintained a certain distance; (4) the systems of ventilation, water, power, and transportation were complete; and (5) the height and width of the roadway met the requirements for drilling. As shown in Figure 5, the first measuring point was located in the South-9 mine haulage roadway, the second measuring point was located in the South-9 haulage roadway, and the third measuring point was arranged in the 72909 ventilation roadway.

3.2.2. Roof Strata Distribution and Structure Observation. The purpose of observing the structure of the surrounding rock is to understand the distribution of roof

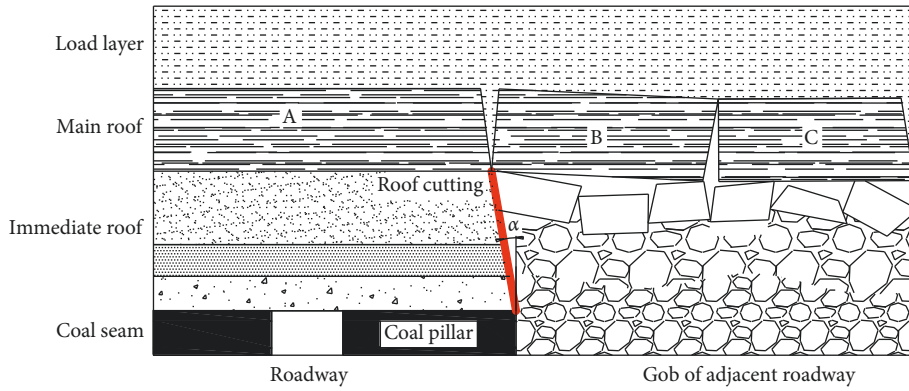


FIGURE 1: Structural model of the short-arm beam.

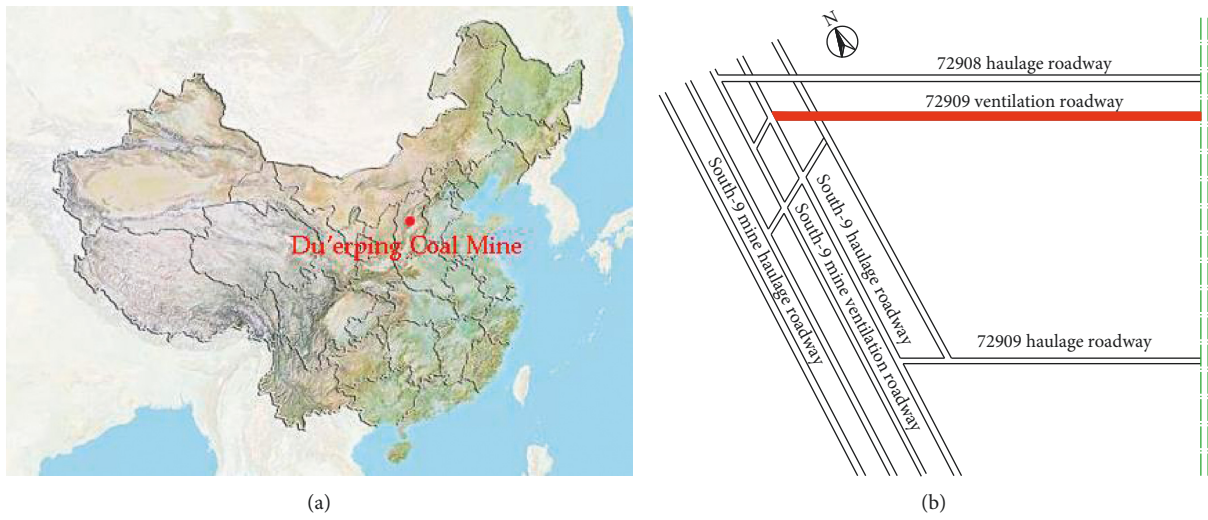


FIGURE 2: Location of (a) Du'erping coal mine and (b) the 72909 ventilation roadway.

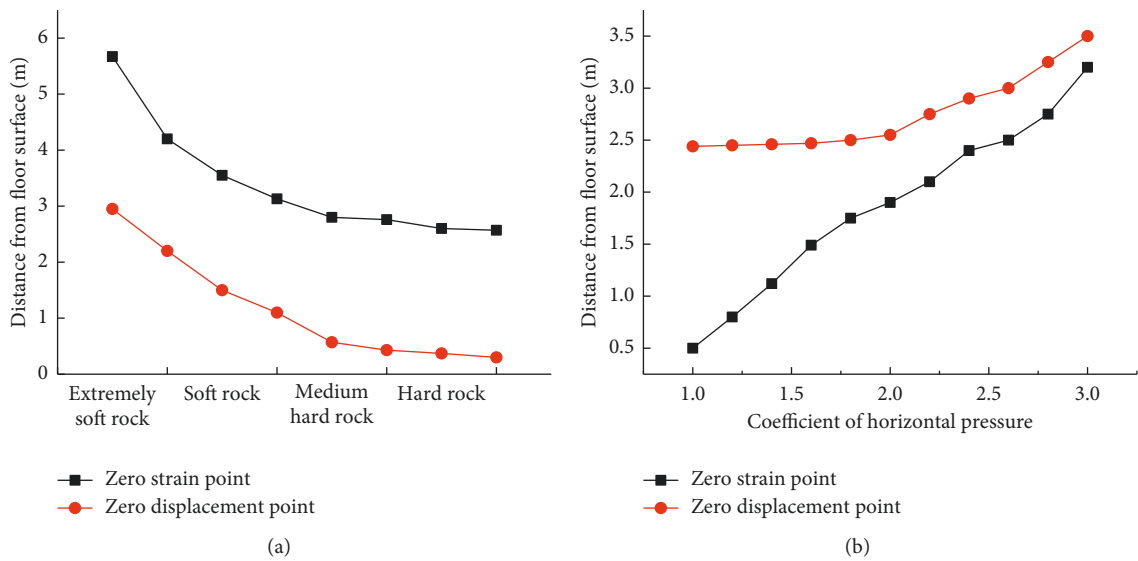


FIGURE 3: Factors influencing floor heave. The influence of (a) floor lithology on floor heave and (b) horizontal stress on floor heave.

TABLE 1: Mechanical parameters of the floor.

Mechanical parameter	Hard rock	Medium-hard rock	Soft rock	Extremely soft rock
Compressive strength (MPa)	≥ 60	30~60	15~30	≤ 15
Cohesion (MPa)	≥ 6.5	4.0~6.5	2.5~4.0	≤ 2.5
Internal friction angle ($^{\circ}$)	≥ 38	30~38	20~30	≤ 20
Strength of extension (MPa)	≥ 4.2	3.2~4.2	2.2~3.2	≤ 2.2
Density ($\text{g}\cdot\text{m}^{-3}$)	≥ 2.4	2.0~2.4	1.6~2.0	≤ 1.6

Thickness (m)	Column	Lithology	Bulk (GPa)	Shear (GPa)	Tension (MPa)	Cohesion (MPa)	Friction angle ($^{\circ}$)	Density ($\text{kg}\cdot\text{m}^{-3}$)
3		Sandy mudstone	1.08	2.05	2.32	2.28	34	2150
1.39		Mudstone	0.97	1.45	1.92	1.88	33	2100
4.91		Sandy mudstone	1.08	2.05	2.32	2.28	34	2150
7.87		Fine sandstone	1.21	2.58	2.92	3.35	36	2300
4.25		Sandy mudstone	1.08	2.05	2.32	2.28	34	2150
0.50		#1 coal	0.81	1.22	1.69	1.71	31	1400
$\frac{2.90 - 1.65}{1.75}$		Fine sandstone	1.21	2.58	2.92	3.35	36	2300
$\frac{2.47 - 1.58}{1.94}$		Siltstone	2.81	3.22	4.53	3.82	41	2460
$\frac{3.50 - 1.90}{2.93}$		#2 coal	0.81	1.22	1.69	1.71	31	1400
$\frac{0.80 - 0.20}{0.60}$		Sandy mudstone	1.08	2.05	2.32	2.28	34	2150
$\frac{1.50 - 0.75}{1.00}$		Fine sandstone	1.21	2.58	2.92	3.35	36	2300
$\frac{0.90 - 0.50}{0.70}$		Mudstone	0.97	1.45	1.92	1.88	33	2100
$\frac{5.05 - 1.40}{1.83}$		Siltstone	2.81	3.22	4.53	3.82	41	2460
$\frac{3.37 - 1.50}{2.10}$		Sandy mudstone	1.08	2.05	2.32	2.28	34	2150
$\frac{0.80 - 0.00}{0.60}$		#3 coal	0.81	1.22	1.69	1.71	31	1400
$\frac{2.85 - 0.30}{1.30}$		Sandy mudstone	1.08	2.05	2.32	2.28	34	2150
$\frac{3.59 - 1.30}{2.30}$		#4 coal	0.81	1.22	1.69	1.71	31	1400

FIGURE 4: Coal seam stratum synthesis histogram.

strata within 25 m and to determine a suitable test section for stress measurement. The borehole observations are shown in Figure 6, and the analysis results are shown in Table 2.

3.2.3. *Ground Stress Measurement.* The ground stress was tested with a SY-56 hydraulic fracturing ground stress measuring device, and the hydraulic fracturing curve is shown in Figure 7.

- (1) The hydraulic fracturing curve of the first measuring point is shown in Figure 7(a).

The calculation is as follows:

$$\begin{aligned} P_{b1} &= 26.82 \text{ MPa}, \\ P_{r1} &= 19.64 \text{ MPa}, \\ P_{s1} &= 18.0 \text{ MPa}. \end{aligned} \quad (1)$$

For the first measuring point, the height of the roadway is 3 m, the depth of the measuring section is 17 m, and the

mining depth of the roadway is 508 m. It can be obtained as follows:

$$\begin{aligned} \sigma_{H1} &= 33.44 \text{ MPa}, \\ \sigma_{h1} &= 17.54 \text{ MPa}, \\ \sigma_{v1} &= 25.40 \text{ MPa}. \end{aligned} \quad (2)$$

- (2) The hydraulic fracturing curve of the second measuring point is shown in Figure 7(b).

The calculation is as follows:

$$\begin{aligned} P_{b2} &= 20.76 \text{ MPa}, \\ P_{r2} &= 14.66 \text{ MPa}, \\ P_{s2} &= 13.60 \text{ MPa}. \end{aligned} \quad (3)$$

For the second measuring point, the height of the roadway is 3.1 m, the depth of the measuring section is 21 m, and the mining depth of the roadway is 630 m. It can be obtained as follows:

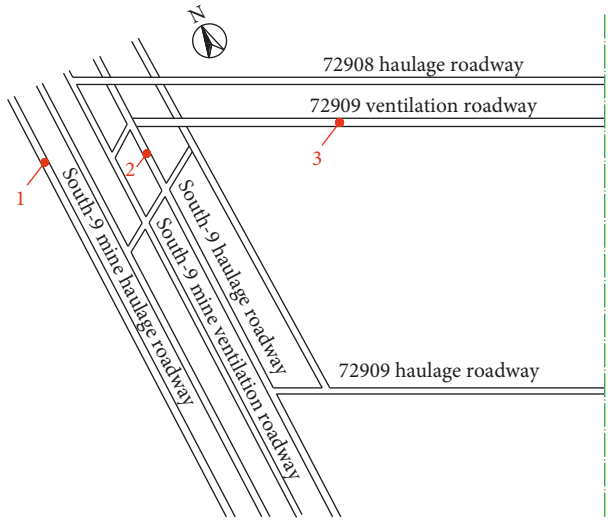


FIGURE 5: Layout of measuring points.

$$\begin{aligned}\sigma_{H2} &= 31.50 \text{ MPa,} \\ \sigma_{h2} &= 13.14 \text{ MPa,} \\ \sigma_{v2} &= 25.22 \text{ MPa.}\end{aligned}\quad (4)$$

- (3) The hydraulic fracturing curve of the third measuring point is shown in Figure 7(c).

The calculation is as follows:

$$\begin{aligned}P_{b3} &= 34.98 \text{ MPa,} \\ P_{r3} &= 28.54 \text{ MPa,} \\ P_{s3} &= 20.96 \text{ MPa.}\end{aligned}\quad (5)$$

For the third measuring point, the height of the roadway is 3 m, the depth of the measuring section is 14.7 m, and the mining depth of the roadway is 608 m. It can be obtained as follows:

$$\begin{aligned}\sigma_{H3} &= 33.62 \text{ MPa,} \\ \sigma_{h3} &= 20.60 \text{ MPa,} \\ \sigma_{v3} &= 30.16 \text{ MPa.}\end{aligned}\quad (6)$$

According to the measurements on the site, the surrounding rock of the #2 coal seam in the Du'erping coal mine is in a high stress field. The maximum and minimum values of the maximum horizontal principal stress are 33.62 MPa and 31.50 MPa, respectively. The maximum and minimum values of the minimum horizontal principal stress are 20.60 MPa and 13.14 MPa, respectively. The maximum and minimum values of the vertical stress are 30.16 MPa and 25.22 MPa, respectively. The type of stress field is $\sigma_H > \sigma_v > \sigma_h$.

3.2.4. The Strength of the Floor Strata Measurement. The borehole penetrating method was used to measure the surrounding rock strength of the floor strata in the 72909 ventilation roadway. Compared with the method of testing

the strength of rock samples in laboratory, the borehole penetrating method can measure not only the rock strength of different depths in floor strata but also the rock layers containing structural planes, such as joints and cracks [27, 28]. Therefore, the measured rock mass strength is more accurate and closer to the actual situation. The rock strength of the rock layers was measured within 10 m of the floor with the WQCZ-56 surrounding rock strength tester. The test results of the surrounding rock strength of the #2 coal seam floor strata are shown in Figure 8.

A comprehensive analysis of the strength test results of the floor strata showed that the floor strata of #2 coal seam in the Du'erping coal mine is mainly mudstone, sandy mudstone, and fine sandstone, and some sandy mudstone rock layers also contain fine sandstone interlayers. Due to the diagenetic process, the thickness of the rock layer is different in different measuring point locations. The strength of the mudstone layer is concentrated at 30–45 MPa, and the average value is 34.22 MPa. The strength of the sandy mudstone layer is concentrated at 45–65 MPa, and the strength is obviously higher than the rock layer at the same depth—the fine sandstone interlayer. The average strength of the sandy mudstone layer is 57.52 MPa, and the average strength of the fine sandstone layer is 80.79 MPa.

3.3. Main Reason for the Floor Heave in the 72909 Ventilation Roadway. According to the hydraulic fracturing experiment, the surrounding rock of the #2 coal seam in the Du'erping coal mine is a high stress field, and the type of stress field is $\sigma_H > \sigma_v > \sigma_h$. According to the strength of the floor strata measurement, the floor strata of the 72909 ventilation roadway are mainly hard rock and medium-hard rock, and there is almost no water in the roadway; therefore, the softening effect of water on the floor strata of the roadway is negligible. The ground stress is the main reason for the floor heave in the 72909 ventilation roadway.

4. Scheme Design for Pressure Relief by Roof Cutting

The essence of pressure relief by roof cutting is the blasting presplitting of the roof strata of the adjacent roadway by the bidirectional energy-cavity blasting technology. After the adjacent working face is mined, the roof strata of the adjacent roadway are cut by the ground pressure. The blasting presplitting cuts the connection in the roof strata between the adjacent working face and the protected roadway, reducing the impact of ground pressure on the protected roadway. Moreover, the fallen gangue supports the overlying main roof strata, controls the rotation and sinking deformation of the main roof strata, and realizes the purpose of pressure relief. Based on the existing research results and field engineering experience [29–31], the height and angle of the roof cutting have a great influence on the effect of pressure relief. A reasonable roof cutting height can completely cut off the roof strata connection between the protected roadway and the gob of the adjacent working face, ensuring that the adjacent working face will not have a great

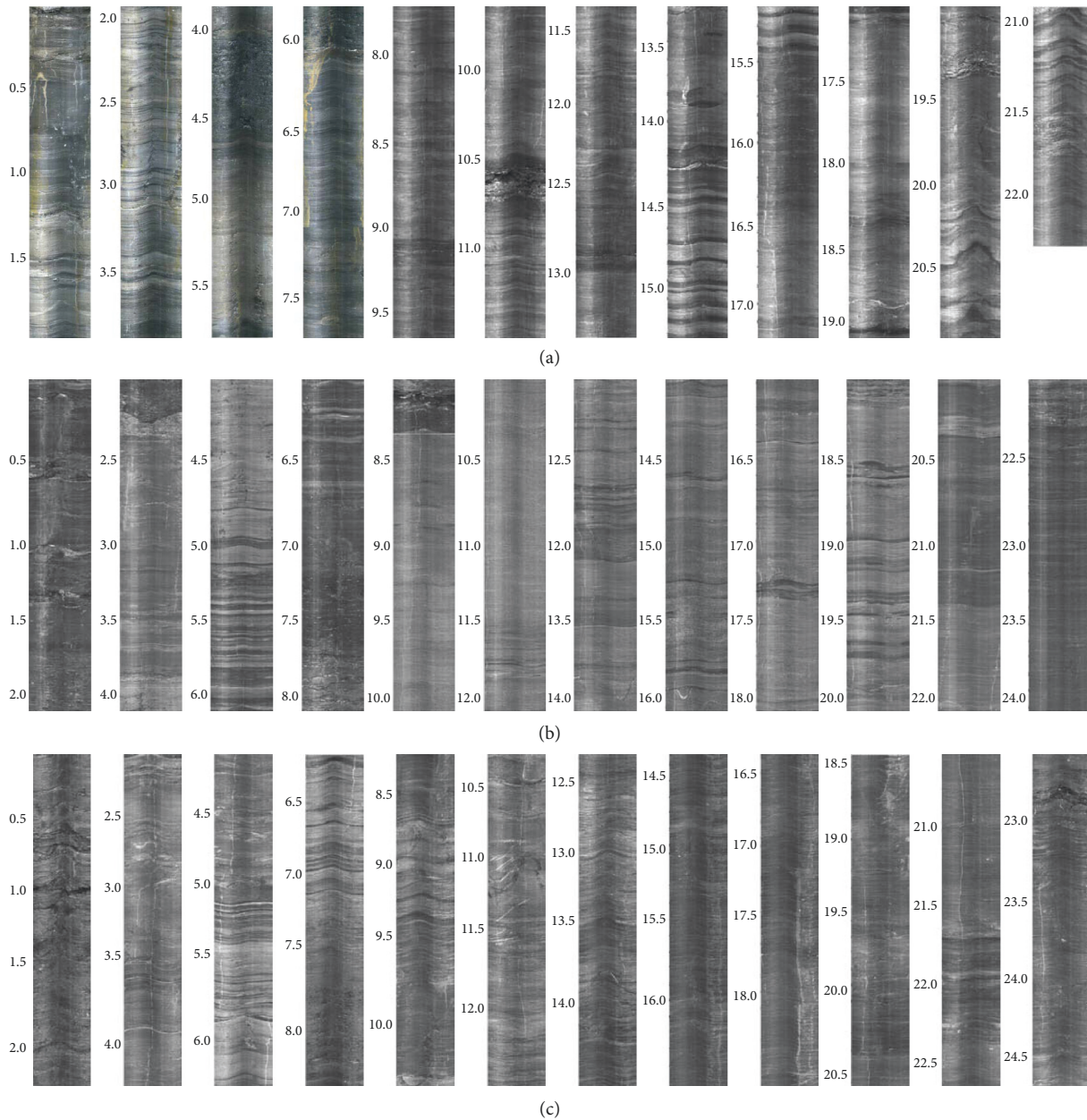


FIGURE 6: Structure observation of the (a) first measuring point, (b) second measuring point, and (c) third measuring point.

TABLE 2: The suitable test section for stress measurement.

Measuring points	The suitable test section for stress measurement
The first measuring point	The 17 m position conforms to the experimental conditions
The second measuring point	The 21 m position conforms to the experimental conditions
The third measuring point	The 14.7 m position conforms to the experimental conditions

impact on the protected roadway. A reasonable angle of roof cutting can also ensure that the roof strata of the adjacent roadway collapse in time, filling in the gob after the working face is mined and supporting the overlying rock strata to

mitigate the impact of the main roof sagging on the protected roadway. The depth and angle of the roof cutting have a great influence on the effect of pressure relief. Therefore, the optimal depth and angle of the roof cutting are key to the “pressure relief by roof cutting in the adjacent roadway” to control roadway deformation.

4.1. Reasonable Design of Roof Cutting Height. In order to improve the stress distribution of the surrounding rock of the 72909 ventilation roadway, directional presplitting blasting of the overlying strata of the adjacent roadway was carried out. The purpose of presplitting blasting had two aspects: one was to cut off the hard overlying strata to cut off the stress propagation path and the other was to promote the

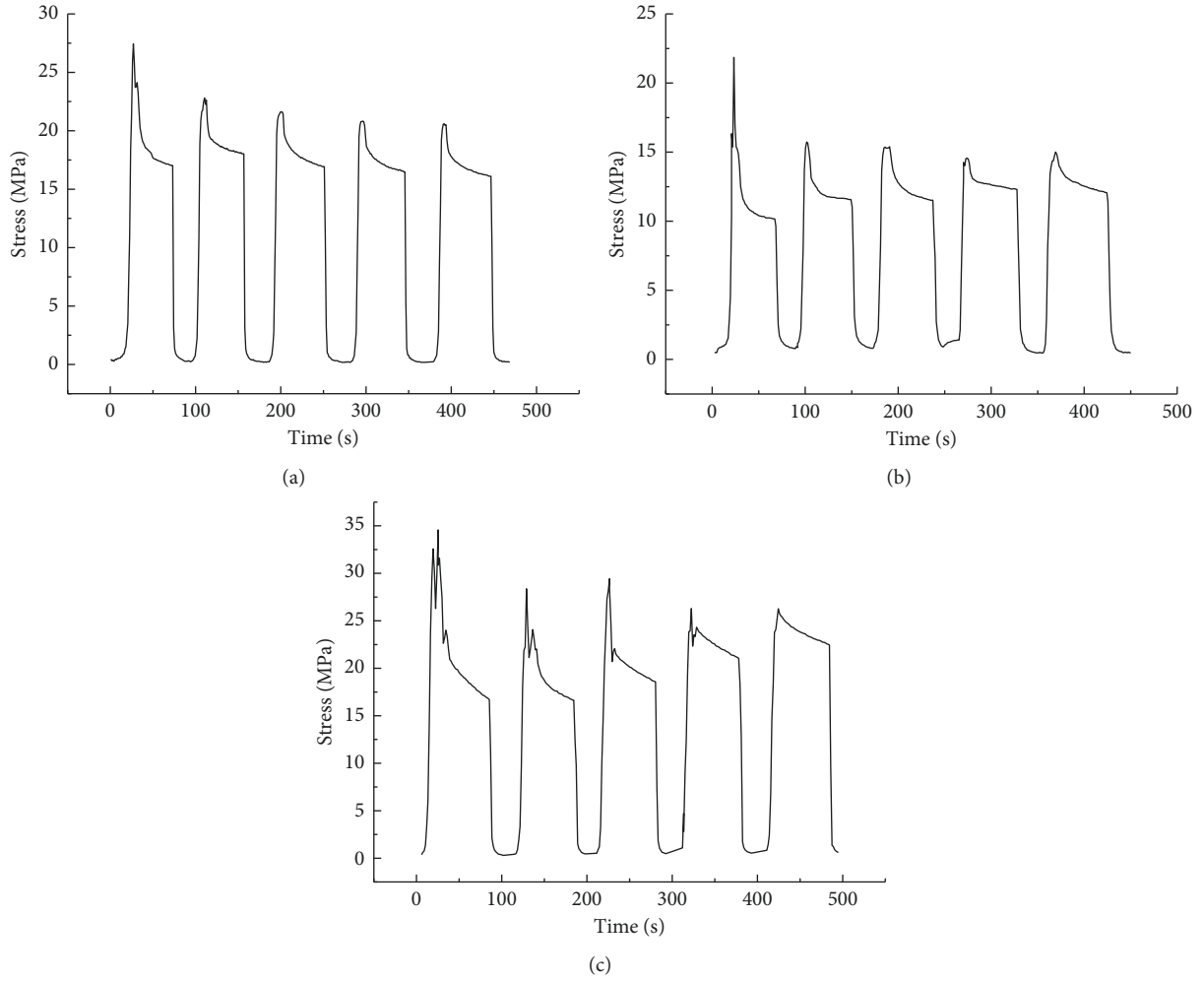


FIGURE 7: Hydraulic fracturing curves of the (a) first measuring point, (b) second measuring point, and (c) third measuring point.

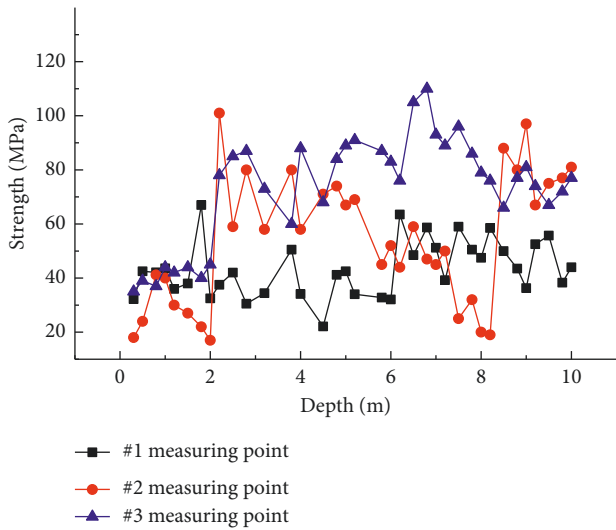


FIGURE 8: Strength curves of the floor strata.

overlying strata collapse and fill the gob in time to support the overlying rock strata and reduce the suspension area. Then, the overlying rock subsidence and the ground pressure

in the roadway were reduced. Thus, the roof cutting height should be determined from the two aspects: one is the location of the hard overlying stratum of the #2 coal seam and the other is that the gob can be filled with the collapsed gangue.

(1) The location of the hard overlying strata.

According to the observations of the roof strata and geological data, there are about eight overlying strata within 25 m of the #2 coal seam.

The hard overlying strata [32] can be judged by equation (7), as follows:

$$\begin{cases} q_1 = \gamma_1 h_1, \\ (qn)1 = \frac{E_1 h_1^3 \sum_{i=1}^n \gamma_i h_i}{\sum_{i=1}^n E_i h_i^n}, \end{cases} \quad (7)$$

where q_1 is the load of the first roof layer in MPa, $(qn)1$ is the load of the n th overlying layer to the first roof layer in MPa, γ is the bulk density of the roof layer in $\text{mN} \cdot \text{m}^{-3}$, h is the thickness of the overlying layer in m, and E is the elasticity modulus in GPa.

When $(qn)1 < (qn-1)1$, the n th overlying layer is the first hard stratum. Then, the load of the overlying layer on the n th overlying layer was calculated with the n th overlying layer as the basal layer. Ultimately, the calculations and analyses determined all the hard overlying strata within 25 m of the #2 coal seam.

The results calculated by equation (7) are as follows:

$$\begin{aligned}
 q1 &= 50.44 \text{ kPa}, \\
 (q2)1 &= 47.26 \text{ kPa}, \\
 q2 &= 41.3 \text{ kPa}, \\
 (q3)2 &= 47.42 \text{ kPa}, \\
 (q4)2 &= 34.46 \text{ kPa}, \\
 q4 &= 93.5 \text{ kPa}, \\
 (q5)4 &= 9.19 \text{ kPa}, \\
 q5 &= 185.73 \text{ kPa}, \\
 (q6)5 &= 279.11 \text{ kPa}, \\
 (q7)5 &= 304.96 \text{ kPa}, \\
 (q8)5 &= 363.43 \text{ kPa}.
 \end{aligned} \tag{8}$$

The above analysis shows that there are three hard rock layers within 25 m above the #2 coal seam. The third hard overlying layer is fine sandstone with a thickness of 7.87 m, and it is away from the #2 coal seam 8.5 m, as shown in Table 3.

To presplit the hard overlying layer to cut off the stress propagation path, the third hard overlying layer should be cut off and the roof cutting height should be about 17 m.

- (2) The thickness of the overlying strata collapse to fill the gob.

The thickness of presplitting the overlying strata required to fill the gob can be calculated by equation (9):

$$H = \frac{H_m - \Delta H_1 - \Delta H_2}{K - 1}, \tag{9}$$

where H is the height of roof cutting in m; H_m is the maximum mining height in m; ΔH_1 is the volume of roof subsidence in m; ΔH_2 is the volume of the floor heave in m; and K is the coefficient of bulk increase of the overlying strata.

To verify the aforementioned calculation results according to the field conditions of the #2 coal seam of the Du'erping coal mine, the following field parameters applied to equation (9) were chosen: $H_m = 3.5$ m and $K = 1.35$. In order to obtain the maximum value of the height of roof cutting, the volumes of roof convergence and floor heave were not taken into consideration, i.e., $\Delta H_1 = \Delta H_2 = 0$. The height of roof cutting was 10 m, which was calculated using equation (9).

In accordance with the aforementioned analysis, the optimal theoretical height of roof cutting is 17 m, not only to cut off the stress transfer but also to ensure that the gob can be filled with the collapsed gangue.

4.2. The Angle of Roof Cutting and Roadway Support. In order to prevent unstable failure of the roof strata of the 72908 haulage roadway after presplitting blasting, the presplitting blasting hole needs to be an angle " α " to ensure that the roof can self-lock and maintain stability after presplitting blasting, but the angle " α " should not be too large to avoid affecting the collapse of the overlying strata. Meanwhile, single props were used in the temporary support and were set at the presplitting blasting side, and the interval of two props was 1000 mm, as shown in Figure 9(a).

According to the Voussoir beam theory and S-R stability principle of the surrounding rock structure, when the fracture surface of the basic rock layer forms a certain angle " α " with the vertical surface, the force relationship of the rock block is as shown in Figure 9(b), and the condition of rock stability is as follows:

$$[T \cos \alpha + (R - F) \sin \alpha] \cdot \tan \varphi = (R - F) \cos \alpha - T \sin \alpha. \tag{10}$$

Equation (10) can be simplified as follows:

$$T \sin(\alpha + \varphi) = (R - F) \cos(\alpha + \varphi), \tag{11}$$

so, $\alpha = \arctan((R - F)/T) - \varphi$:

$$\begin{cases} f = \tau \times h \times 1, \\ R = \rho g h d, \end{cases} \tag{12}$$

where T is the horizontal force of the rock block in kN; R is the load of block B in kN; F is the working resistance of a single prop in kN; h is the height of roof cutting in m; φ is the friction angle of the rock block in $^\circ$; α is the angle of the presplitting blasting borehole in $^\circ$; f is the shear force of the rock block in kN; ρ is the density of the rock strata in kg/m^3 ; and d is the width of the roadway in m.

For convenient calculation, a component of T can be approximated as f where " $f = T \sin \alpha$ ". According to the actual conditions of the 72908 haulage roadway, the field parameters were chosen as follows: $\varphi = 27^\circ$, $\tau = 0.13$ MPa, $\rho = 2500$ kg/m^3 , $h = 17$ m, and $d = 4.2$ m.

According to the aforementioned theoretical calculation, when the angle of the presplitting blasting borehole is in the range of 10° to 15° , the roof strata of the roadway can remain stable. The smaller the angle of the presplitting blasting borehole is, the smaller the drilling depth required to cut off the hard rock layer is, the smaller the amount of work is, and the easier it is for the roof strata to fall. Thus, the angle of the presplitting blasting borehole was set at 10° . Under this condition, the working resistance of a single prop was about 180 kN, and a row of single props set at the presplitting blasting side was able to meet the requirements for stability maintenance of the roof strata.

4.3. Numerical Simulation. A numerical model was established according to the geological conditions of the #2 coal seam in the Du'erping coal mine. The mechanical parameters of the roof and floor rock strata are shown in Figure 3. The model length, width, and height were $565 \times 300 \times 60$ m; the vertical boundary force was applied to the upper

TABLE 3: Overlying layers of #2 coal seam.

Location	Lithology	Thickness (m)	Remark
8	Sandy mudstone	3	
7	Mudstone	1.39	
6	Sandy mudstone	4.91	
5	Fine sandstone	7.87	The third hard overlying layer
4	Sandy mudstone	4.25	The second hard overlying layer
3	1# coal seam	0.5	
2	Fine sandstone	1.75	The first hard overlying layer
1	Siltstone	1.94	

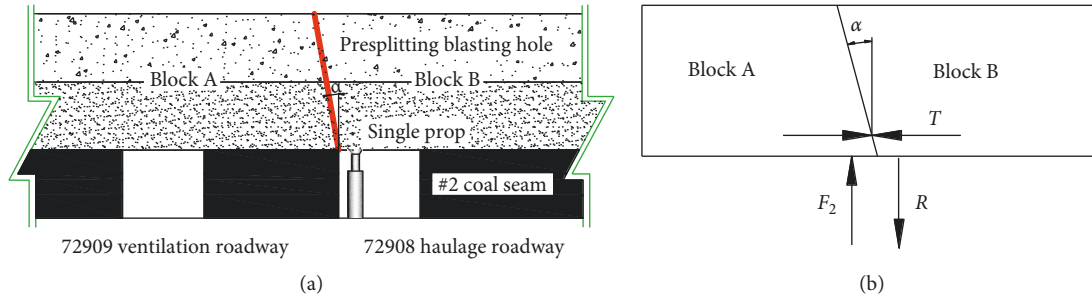


FIGURE 9: (a) Presplitting blasting borehole and temporary support and (b) the approximate stress situation of block B.

boundary; the lower boundary was fixed in the vertical direction; and the front, rear, left, and right boundaries were fixed in the horizontal direction. The width of the simulated working face was 212 m, the thickness of the coal seam was 2.0 m, and the width and height of the roadway were 4.0×2.0 m. A 25 m protective coal pillar was placed between the 72909 working face and the 72908 working face. After the 72908 working face was mined, the horizontal section of the vertical stress distribution of the 72909 working face at 20 m was determined and is shown in Figure 10. The roof strata of the 72908 haulage roadway without presplitting blasting is shown in Figure 10(a), and the roof strata of the 72908 haulage roadway with presplitting blasting is shown in Figure 10(b).

Figure 10 shows whether presplitting blasting the roof strata of the 72908 haulage roadway had a great influence on the stress distribution of the surrounding rock. As shown in Figure 10(a), for the roof strata of the 72908 haulage roadway without presplitting blasting, the 72908 haulage roadway and 72909 ventilation roadway both had a concentration of stress in the ribs. The maximum values of stress in the coal pillar side and working face side of the 72909 ventilation roadway were 30.1 MPa and 31.5 MPa, respectively. As shown in Figure 10(b), for the roof strata of the 72908 haulage roadway with presplitting blasting, there was almost no stress concentration in the coal pillar, and the stress concentration transferred to the depth of the working face coal mass. The maximum values of stress in the coal pillar side and working face side of the 72909 ventilation roadway were 16.8 MPa and 18.3 MPa, respectively. After presplitting blasting the roof strata, the maximum value of stress in the coal pillar side and working face side of the 72909 ventilation roadway were reduced by 44.2% and 41.9%, respectively.

As shown in Figure 10, at about 20 m in front of the 72909 working face, a concentration of stress occurred in the two ribs of the 72909 ventilation roadway. Therefore, the vertical section of the vertical stress was selected 20 m ahead of the 72909 working face. The vertical section of the vertical stress for the roof strata of the 72908 haulage roadway without presplitting blasting is shown in Figure 11(a), and the roof strata of the 72908 haulage roadway with presplitting blasting is shown in Figure 11(b).

As shown in Figure 11(a), the stress concentration was about 5 m in the working face side of the 72909 ventilation roadway, the maximum value of stress was 29.8 MPa, and the maximum value of stress in the coal pillar side was 17.5 MPa. As shown in Figure 11(b), since the presplitting blasting cuts off the stress propagation path, the stress concentration area of the 72909 ventilation roadway was transferred to the depth of the working face coal mass. The maximum value of stress in the working face side was 15.5 MPa, and the maximum value of stress in the coal pillar side was 12.4 MPa; these were reduced by 47.9% and 29.1%, respectively.

As shown in Figure 1, when the presplitting blasting was carried out on the roof strata of the adjacent roadway, the hard overlying strata were cut off, and the roof strata fell and filled the gob, which could have supported the overlying strata and reduced the disturbance of mining to the roadway.

According to the above analysis, roof cutting in the adjacent roadway cut off the stress propagation path; thus, the stress concentration was forced to transfer to the deep part of the coal mass, so the surrounding rock stress of the roadway was reduced, and the mechanical environment of the surrounding rock of the roadway was improved. The problem of roadway deformation caused by stress was fundamentally solved. Therefore, in theory, the presplitting blasting of the roof strata of the adjacent roadway can

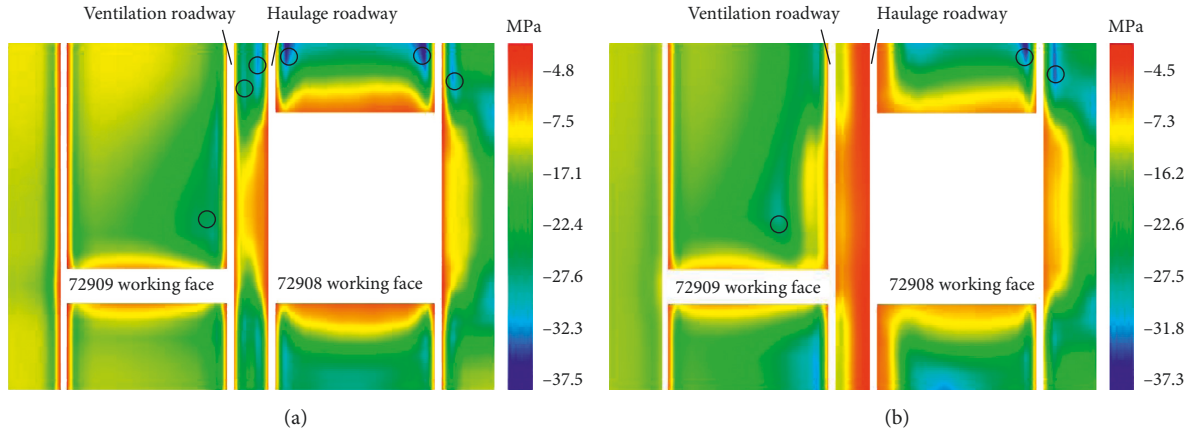


FIGURE 10: Vertical stress distribution of the roof strata of the 72908 haulage roadway (a) without presplitting blasting and (b) with presplitting blasting.

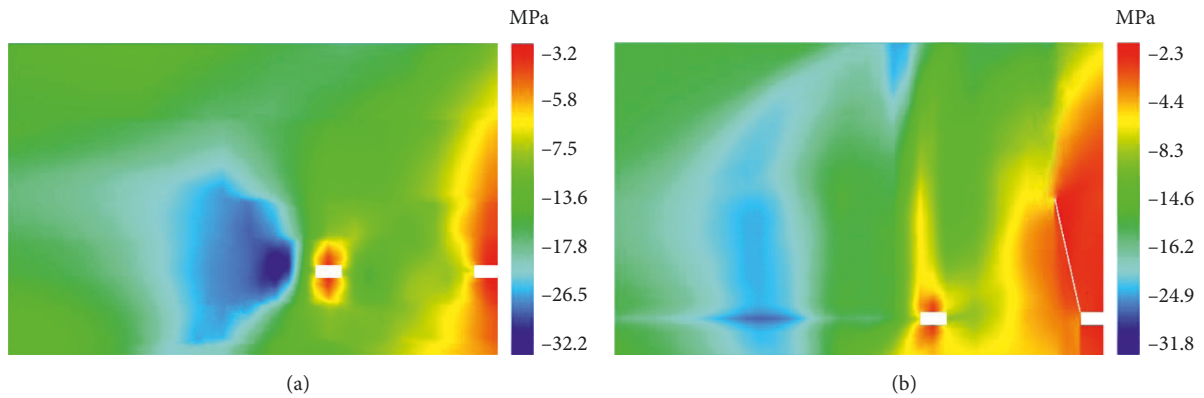


FIGURE 11: Vertical stress distribution of the roof strata of the 72908 haulage roadway (a) without presplitting blasting and (b) with presplitting blasting.

improve the stress of the surrounding rock of the roadway and reduce the stress of the surrounding rock, so that the size of the protective coal pillar between the working faces reduces, improving the coal recovery rate and reducing resource waste.

5. Determination of the Best Blasting Parameters

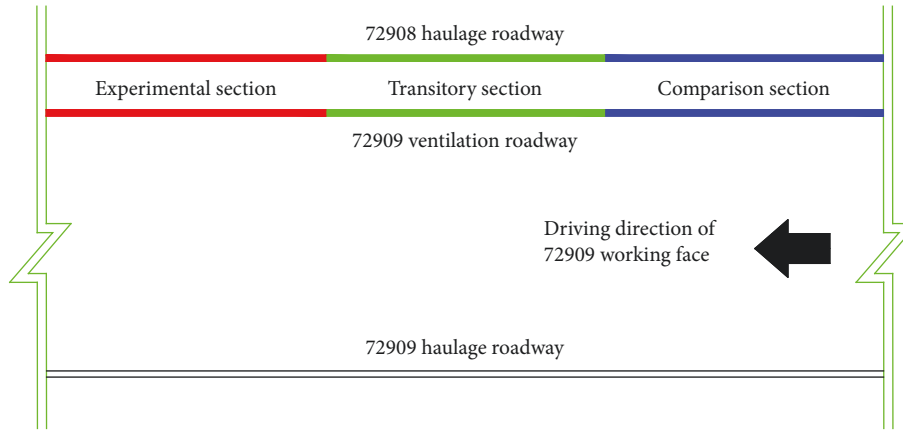
In order to verify the effect that roof cutting in the adjacent roadway to control the roadway deformation, 300 m of the 72908 haulage roadway was selected as the test section, and it was divided into three sections along the driving direction of the working face—each section is 100 m long. As seen in Figure 12(a), the first section was the comparison section without presplitting blasting, the second section was the transitory section used to determine the best blasting parameters, the third section was the experimental section with presplitting blasting with the best blasting parameters. The presplitting blasting of the overlying strata on the 72908 haulage roadway is shown in Figure 12(b).

According to previous engineering experience [33–35], the space between the presplitting blasting borehole is

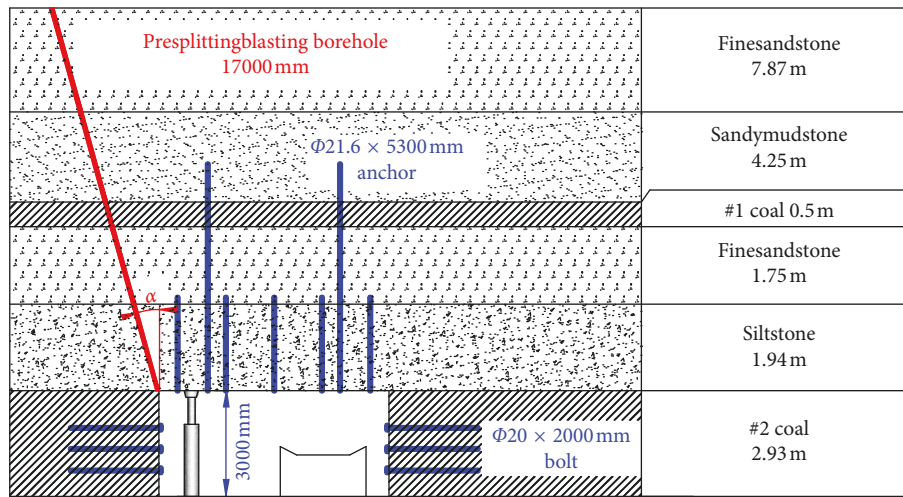
generally in the range of 400–600 mm. The numerical simulation was carried out on the rock strata conditions of the #2 coal seam in Du'erping coal mine. The LS-DYNA software was used to numerically analyze the presplitting blasting borehole spaces of 400 mm, 500 mm, and 600 mm to determine the optimal space of the borehole. The results are shown in Figure 13.

As shown in Figure 13, when the space between the presplitting blasting borehole was 400 mm, the stress superposition was too strong and easily caused the borehole to collapse. When the space between the presplitting blasting borehole was 500 mm, the stress superposition was strong enough to run through the roof strata. When the space between the presplitting blasting borehole was 600 mm, the stress superposition was too feeble to run through the roof strata. Based on the numerical simulation, considering the previous engineering experience and engineering quantity, the space between the presplitting blasting borehole was selected to be 500 mm.

In order to ensure the effect of presplitting blasting, a selection of 100 m in the 72908 haulage roadway was chosen to be the transitory section for the blasting experiment and the optimum blasting parameters were



(a)



(b)

FIGURE 12: (a) Partition of test section and (b) presplitting blasting in the 72908 haulage roadway.

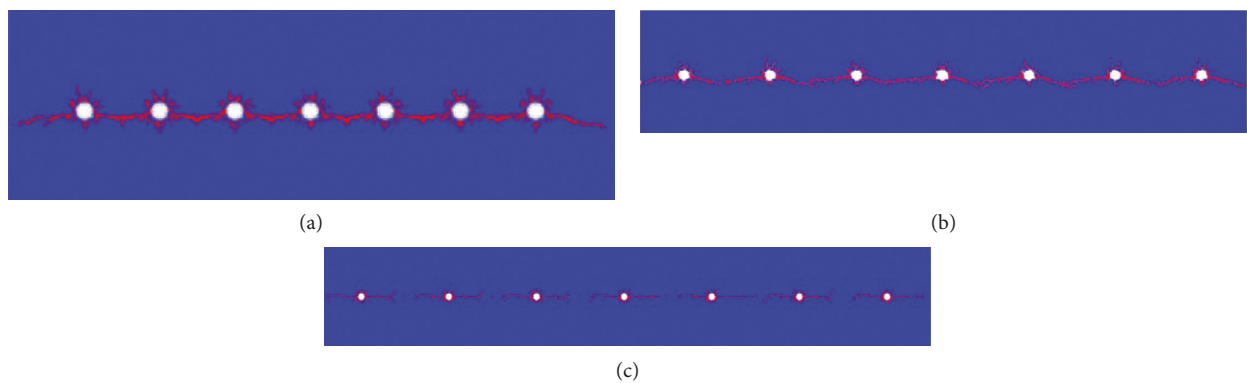


FIGURE 13: The presplitting blasting borehole spacing of (a) 400 mm, (b) 500 mm, and (c) 600 mm.

selected. According to the aforementioned analysis, the presplitting blasting borehole had an interval of 500 mm, a length of 17 m, and an angle with the vertical direction of 10°. The length of the binding energy tube was 1.5 m, and each presplitting blasting borehole had nine binding energy tubes. The length of the lute was 3.5 m. The experimental

schemes for the blasting experiment are shown in Table 4. The experimental schemes for the blasting methods are shown in Figure 14.

The observations of the blasting effect are shown in Figure 15. As shown in Figures 15(a)–15(c), in schemes 1–3, there were almost no crevices in the observant borehole. As

TABLE 4: Experimental schemes for the volume of explosives.

Scheme	Volume of explosives	Blasting method
1	3+3+3+3+3+2+2+2+1	Single-borehole blasting interval one hole
2	4+3+3+3+3+2+2+2+1	Double-borehole blasting interval one hole
3	4+4+3+3+3+2+2+2+1	Three-borehole blasting interval one hole
4	4+4+3+3+3+2+2+2+2	Four-borehole blasting interval one hole
5	4+4+3+3+3+2+2+2+2	Five-borehole blasting interval one hole

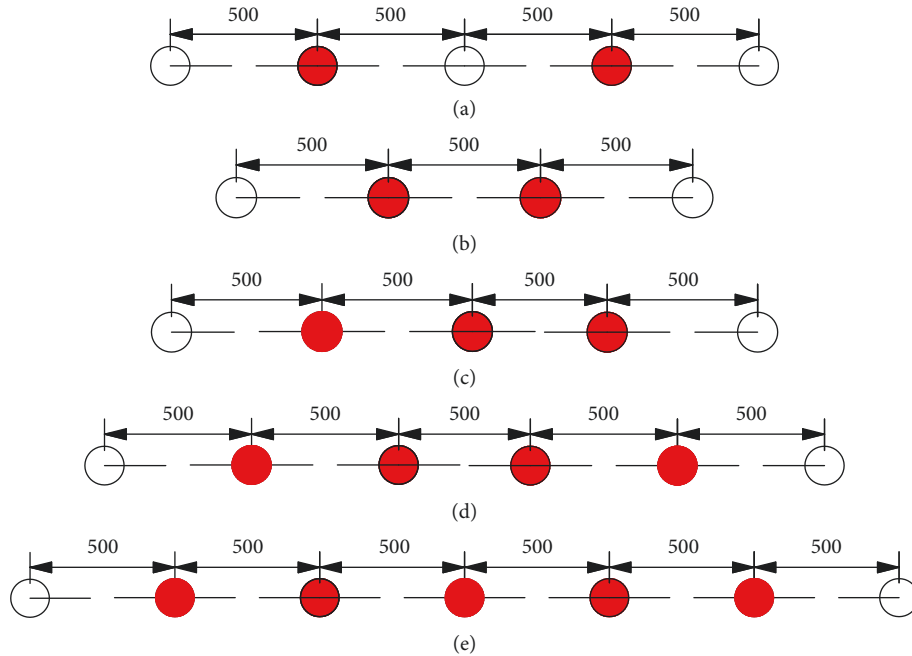


FIGURE 14: The experimental schemes for the blasting methods. (a) Single-borehole blasting interval one hole. (b) Double-borehole blasting interval one hole. (c) Three-borehole blasting interval one hole. (d) Four-borehole blasting interval one hole. (e) Five-borehole blasting interval one hole.

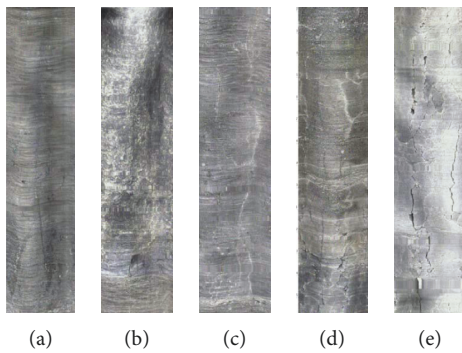


FIGURE 15: The observations of the blasting effect. (a) scheme 1; (b) scheme 2; (c) scheme 3; (d) scheme 4; (e) scheme 5.

shown in Figure 15(d), in scheme 4, there were a few crevices in the observant borehole. As shown in Figure 15(e), in scheme 5, there were many crevices throughout the observant borehole. Thus, the optimum blasting parameters were those in scheme 5, the optimum charge structures are shown in Figure 16, and the optimum blasting method is shown in Figure 14(e).

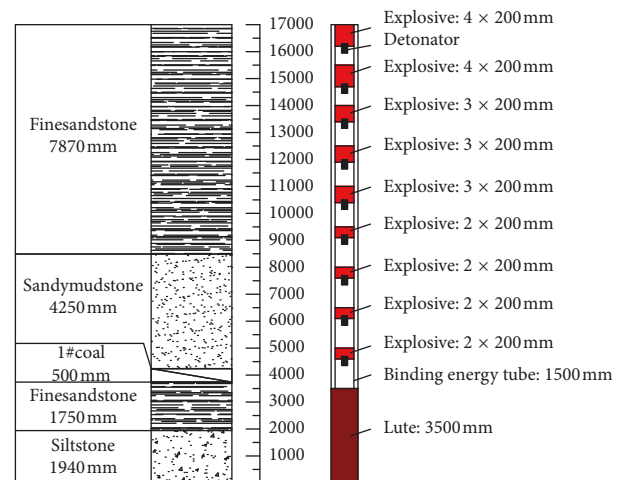


FIGURE 16: The optimum volume of explosives.

6. Engineering Application

Based on the design scheme, a 300 m section in the 72908 haulage roadway was chosen as the test section. In order to

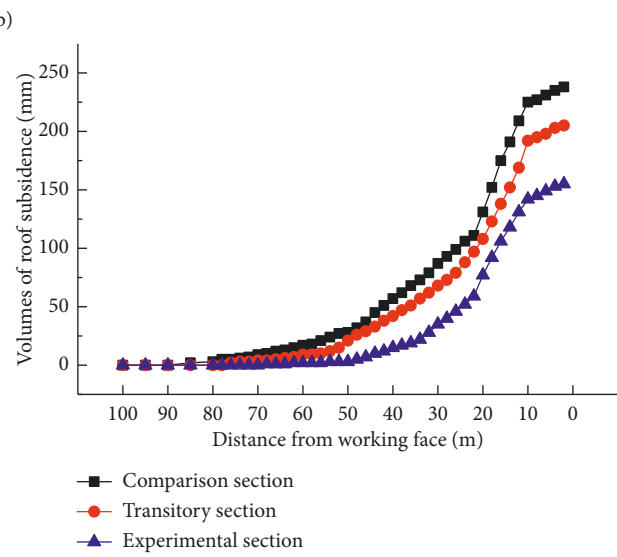
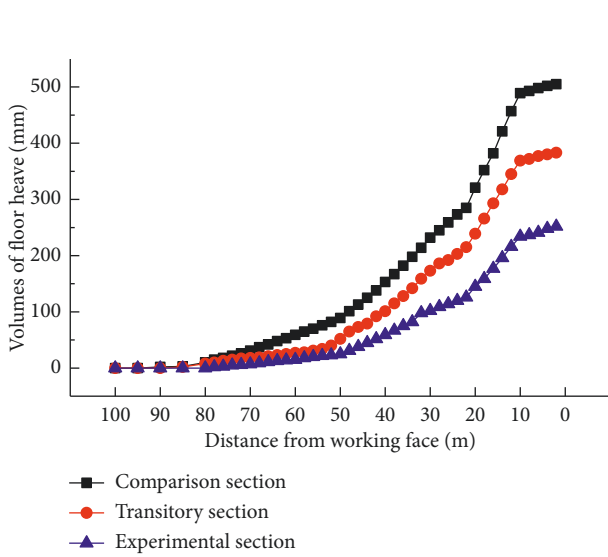
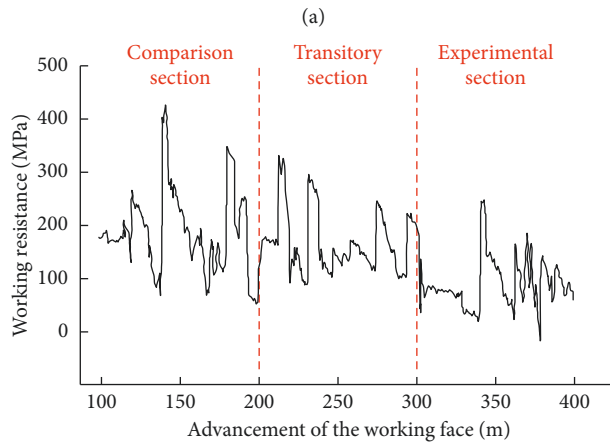
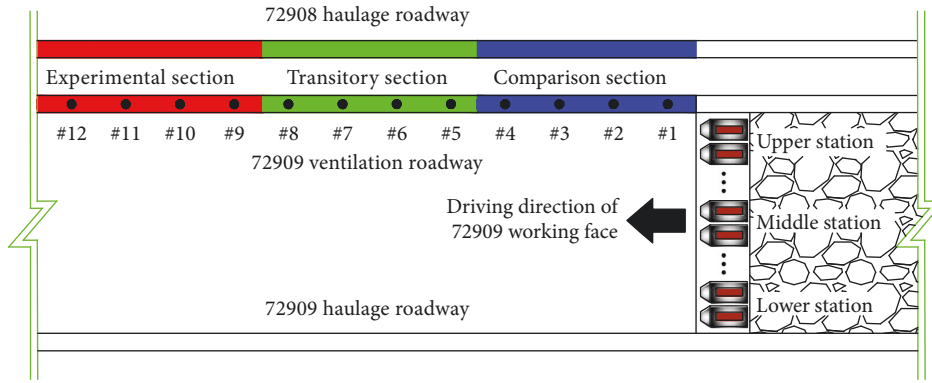


FIGURE 17: Continued.

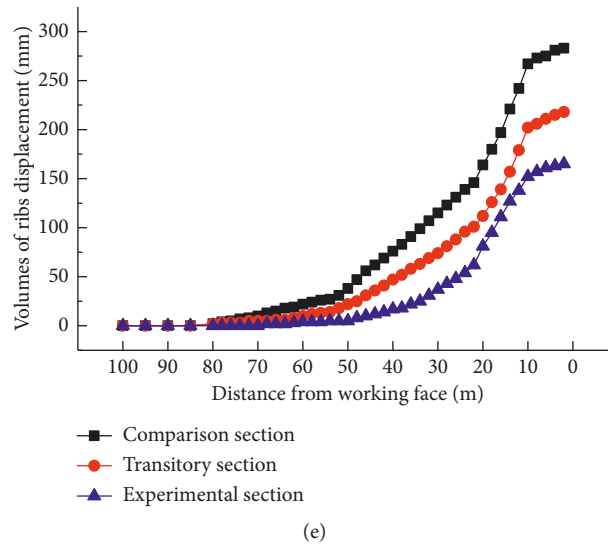


FIGURE 17: Monitoring on the site: (a) layout of the monitoring points. Monitoring curves of (b) the working resistance in the upper station, (c) the floor heave, (d) the roof subsidence, and (e) the rib displacement.

ensure the roadway deformation was adequate, the test section was from the open cut to 100–400 m, the presplitting blasting borehole was on the pillar side of the 72908 haulage roadway, and the length and angle of presplitting blasting borehole were set as 17.0 m and 10° , respectively. The division of the test section in the 72909 ventilation roadway was in accordance with the test section divided in the 72908 haulage roadway. The comparison section was from the open cut to 100–200 m, the transitory section was from the open cut to 200–300 m, and the experimental section was from the open cut to 300–400 m. In order to analyze the effect of pressure relief by roof cutting the adjacent roadway to control roadway deformation, the working resistance of the hydraulic support of 72909 working face and the volume of the roadway deformation of the 72909 ventilation roadway were monitored on the site. The layout of monitoring points is shown in Figure 17(a). At both ends and in the middle of the working face, five measuring points were set and recorded as the upper station, middle station, and lower station, respectively. In order to research the effect of pressure relief by presplitting blasting the roof strata of the adjacent roadway, we focused on the monitoring curve of the upper station, as shown in Figure 17(b). In the 72909 ventilation roadway, twelve monitoring points were set to monitor the volume of roadway deformation, and every 25 m, a monitoring point was set. The monitoring curves of the floor heave, roof subsidence, and rib displacement are shown in Figures 17(c)–17(e), respectively.

As seen in Figure 17(b), in the comparison section, the maximal working resistance of the hydraulic support was 36.5 MPa; in the transitory section, the maximal working resistance of the hydraulic support was 32.1 MPa; and in the experimental section, the maximal working resistance of the hydraulic support was 27.4 MPa. Compared with the comparison section, the pressure peaks of the transitory section and experimental section were reduced by 12.1% and 24.9%, respectively. The effect of pressure relief was

obviously shown by cutting off the roof of the adjacent roadway. As shown in Figure 17(c), the average volumes of the maximum floor heave in the comparison section, transitory section, and experimental section were 505 mm, 383 mm, and 252 mm, respectively. Compared with the comparison section, the average volumes of the maximum floor heave in the transitory section and experimental section were reduced by 24.2% and 50.1%, respectively. As shown in Figure 17(d), the average volumes of the maximum roof subsidence in the comparison section, transitory section, and experimental section were 238 mm, 205 mm, and 155 mm, respectively. Compared with the comparison section, the average volumes of the maximum roof subsidence in the transitory section and experimental section were reduced by 13.9% and 34.9%. As shown in Figure 17(e), the average volumes of the maximum ribs displacement in the comparison section, transitory section, and experimental section were 283 mm, 218 mm, and 165 mm, respectively. Compared with the comparison section, the average volumes of the maximum rib displacement in the transitory section and experimental section were reduced by 22.9% and 41.7%, respectively. Based on in situ measurements and tests, cutting off the roof of the adjacent roadway controlled the roadway deformation satisfactorily.

7. Conclusions

The surrounding rock of the #2 coal seam in the Du'erping coal mine is in a high stress field, and the ground stress is the main reason for the roadway deformation of the 72909 ventilation roadway.

This study proposes a new method to control the roadway deformation caused by high ground stress. Presplitting blasting the hard roof strata of the adjacent roadway to cut off the stress propagation path to reduce the stress on the protected roadway and encourages the roof strata to fall down and fill the gob, reducing the disturbance from the

collapse of the roof strata to the surrounding rock of the protected roadway. This achieves the purpose of controlling the deformation of the roadway.

Based on in situ measurements and tests, the effect of presplitting blasting the roof strata of the adjacent roadway on the roadway deformation caused by high ground stress is significant and provides a successful experience for other coal mines.

Data Availability

All data included in this study are available upon request by contact with the corresponding author.

Conflicts of Interest

The authors declare no conflicts of interest.

Authors' Contributions

Chaowen Hu, Xiaojie Yang, and Manchao He were responsible for conceptualization of the study; Chaowen Hu was responsible for methodology; Chaowen Hu and Yubo Zhou were responsible for software; Chaowen Hu and Haohao Wang performed the formal analysis; Chaowen Hu and Enze Zhen investigated the study; Chaowen Hu, Yubo Zhou, and Haohao Wang involved in data curation; and English editing was done by Xiaoyu Liu and Xingen Ma.

Acknowledgments

This work was supported by the National Natural Science Foundation of China (No. 41672347) and the Natural Science Foundation of Beijing (No. 8142032), which are gratefully acknowledged.

References

- [1] S. Liang, D. Elsworth, X. H. Li, X. H. Fu, and B. Y. Sun, "Key strata characteristics controlling the integrity of deep wells in longwall mining areas," *International Journal of Rock Mechanics and Mining Sciences*, vol. 1, no. 12, pp. 1–28, 2012.
- [2] A. Y. Cao, L. M. Dou, C. B. Wang, and X. X. Yao, "Microseismic precursory characteristics of rock burst hazard in mining areas near a large residual coal pillar: a case study from Xuzhuang coal mine, Xuzhou, China," *Rock Mechanics and Rock Engineering*, vol. 1, no. 7, pp. 12–28, 2016.
- [3] B. Yu, Z. Y. Zhang, T. J. Kuang, and J. L. Liu, "Stress changes and deformation monitoring of longwall coal pillars located in weak ground," *Rock Mechanics and Rock Engineering*, vol. 49, no. 8, pp. 3293–3305, 2016.
- [4] W. Zhang, Z. He, D. Zhang, D. Qi, and W. Zhang, "Surrounding rock deformation control of asymmetrical roadway in deep three-soft coal seam: a case study," *Journal of Geophysics and Engineering*, vol. 15, no. 5, pp. 1917–1928, 2018.
- [5] Y. L. Zhao, L. Y. Zhang, W. J. Wang, J. Z. Tang, H. Lin, and W. Wan, "Transient pulse test and morphological analysis of single rock fractures," *International Journal of Rock Mechanics and Mining Sciences*, vol. 91, no. 1, pp. 139–154, 2018, <https://search.crossref.org/?q=Transient+pulse+test+and+morphological+analysis+of+single+rock+fractures>.
- [6] S. Q. Yang, M. Chen, H. W. Jing, K. F. Chen, and B. Meng, "A case study on large deformation failure mechanism of deep soft rock roadway in Xin'An coal mine, China," *Engineering Geology*, vol. 12, no. 12, pp. 52–65, 2016.
- [7] Y. Yuan, W. Wang, S. Li, and Y. Zhu, "Failure mechanism for surrounding rock of deep circular roadway in coal mine based on mining-induced plastic zone," *Advances in Civil Engineering*, vol. 2018, Article ID 1835381, 14 pages, 2018.
- [8] Y. Zhao, Y. Wang, W. Wang, W. Wan, and J. Tang, "Modeling of non-linear rheological behavior of hard rock using triaxial rheological experiment," *International Journal of Rock Mechanics and Mining Sciences*, vol. 93, no. 3, pp. 66–75, 2017.
- [9] Y. L. Zhao, L. Y. Zhang, W. J. Wang, W. Wan, and W. H. Ma, "Separation of elastoviscoplastic strains of rock and a non-linear creep model," *International Journal of Geomechanics*, vol. 18, no. 1, article 04017129, 2018.
- [10] C. H. Du, P. Cao, Y. Chen, J. Liu, Y. L. Zhao, and J. S. Liu, "Study on the stability and deformation of the roadway subjected to high in-situ stresses," *Geotechnical and Geological Engineering*, vol. 35, no. 4, pp. 1615–1628, 2017.
- [11] G. Guo, H. Kang, D. Qian, F. Gao, and Y. Wang, "Mechanism for controlling floor heave of mining roadways using reinforcing roof and sidewalls in underground coal mine," *Sustainability*, vol. 10, no. 5, pp. 1413–1428, 2018.
- [12] C. K. Liu, J. X. Ren, B. L. Gao, and Y. J. Song, "Support design and practice for floor heave of deeply buried roadway," *Earth and Environmental Science*, vol. 64, no. 1, pp. 32–39, 2017.
- [13] M. C. He, G. L. Zhu, and Z. B. Guo, "Longwall mining 'cutting cantilever beam theory' and 110 mining method in China—the third mining science innovation," *Journal of Rock Mechanics and Geotechnical Engineering*, vol. 7, no. 5, pp. 483–492, 2015.
- [14] Q. Wang, M. C. He, J. Yang, H. K. Gao, B. Jiang, and H. C. Yu, "Study of a no-pillar mining technique with automatically formed gob-side entry retaining for longwall mining in coal mines," *International Journal of Rock Mechanics and Mining Sciences*, vol. 110, pp. 1–8, 2018.
- [15] Y. Wang, Y. Gao, E. Wang, M. He, and J. Yang, "Roof deformation characteristics and preventive techniques using a novel non-pillar mining method of gob-side entry retaining by roof cutting," *Energies*, vol. 11, no. 3, pp. 627–644, 2018.
- [16] Z. G. Tao, Z. G. Song, M. C. He, Z. G. Meng, and S. H. Pang, "Principles of the roof cut short-arm beam mining method (110 method) and its mining-induced stress distribution," *International Journal of Mining Science and Technology*, vol. 28, no. 3, pp. 391–396, 2018.
- [17] Y. G. Hu, W. B. Lu, M. Chen, P. Yan, and J. H. Yang, "Comparison of blast-induced damage between presplit and smooth blasting of high rock slope," *Rock Mechanics and Rock Engineering*, vol. 47, no. 4, pp. 1307–1320, 2014.
- [18] B. Chen, C. Liu, and J. Yang, "Design and application of blasting parameters for presplitting hard roof with the aid of empty-hole effect," *Shock and Vibration*, vol. 2018, Article ID 8749415, 16 pages, 2018.
- [19] B. Huang, P. Li, J. Ma, and S. Chen, "Experimental investigation on the basic law of hydraulic fracturing after water pressure control blasting," *Rock Mechanics and Rock Engineering*, vol. 47, no. 4, pp. 1321–1334, 2013.
- [20] S. Yan, T. Liu, J. Bai, and W. Wu, "Key parameters of gob-side entry retaining in a gassy and thin coal seam with hard roof," *Processes*, vol. 6, no. 5, pp. 51–65, 2018.
- [21] B. T. Shen, "Coal mine roadway stability in soft rock: a case study," *Rock Mechanics and Rock Engineering*, vol. 47, no. 6, pp. 2225–2238, 2013.

- [22] A. X. Wu, S. M. Shun, Y. M. Wang, and X. Chen, "Failure mechanism and supporting measures for large deformation of soft rock roadway in Baluba copper mine," *Archives of Mining Sciences*, vol. 63, no. 2, pp. 449–464, 2018.
- [23] P. Gong, Z. Ma, X. Ni, and R. Zhang, "Floor heave mechanism of gob-side entry retaining with fully-mechanized backfilling mining," *Energies*, vol. 10, no. 12, pp. 2085–2104, 2017.
- [24] X.-R. Meng, R. Peng, G.-M. Zhao, and Y.-M. Li, "Roadway engineering mechanical properties and roadway structural instability mechanisms in deep wells," *KSCE Journal of Civil Engineering*, vol. 22, no. 5, pp. 1954–1966, 2017.
- [25] Y. D. Jiang, W. G. Liu, Y. X. Zhao et al., "Study on surrounding rock stability of deep mining in Kailuan mining group," *Chinese Journal of Rock Mechanics and Engineering*, vol. 24, no. 11, pp. 1857–1862, 2005.
- [26] J. B. Bai, W. F. Li, X. Y. Wang, Y. Xu, and L. J. Huo, "Mechanism of floor heave and control technology of roadway induced by mining," *Journal of Mining and Safety Engineering*, vol. 28, no. 1, pp. 1–5, 2011.
- [27] D. J. Armaghani, M. Hajihassani, B. Y. Bejarbaneh, A. Marto, and E. T. Mohamad, "Indirect measure of shale shear strength parameters by means of rock index tests through an optimized artificial neural network," *Measurement*, vol. 55, no. 6, pp. 487–498, 2014.
- [28] X. Wang, Z. Wen, Y. Jiang, and H. Huang, "Experimental study on mechanical and acoustic emission characteristics of rock-like material under non-uniformly distributed loads," *Rock Mechanics and Rock Engineering*, vol. 51, no. 3, pp. 729–745, 2017.
- [29] H. Hu, L. M. Dou, J. Fan, T. T. Du, and X. L. Sun, "Deep-hole directional fracturing of thick hard roof for rockburst prevention," *Tunnelling and Underground Space Technology*, vol. 32, no. 11, pp. 34–43, 2012.
- [30] Q. Ye, Z. Jia, and C. Zheng, "Study on hydraulic-controlled blasting technology for pressure relief and permeability improvement in a deep hole," *Journal of Petroleum Science and Engineering*, vol. 159, no. 11, pp. 433–442, 2017.
- [31] J. Guo, L. Ma, Y. Wang, and F. Wang, "Hanging wall pressure relief mechanism of horizontal section Top-coal caving face and its application-A case study of the Urumqi Coalfield, China," *Energies*, vol. 10, no. 9, pp. 1371–1391, 2017.
- [32] J. Xue, H. Wang, W. Zhou, B. Ren, C. Duan, and D. Deng, "Experimental research on overlying strata movement and fracture evolution in pillarless stress-relief mining," *International Journal of Coal Science and Technology*, vol. 2, no. 1, pp. 38–45, 2015.
- [33] L. Ma, K. Li, S. Xiao, X. Ding, and S. Chinyanta, "Research on effects of blast casting vibration and vibration absorption of presplitting blasting in open cast mine," *Shock and Vibration*, vol. 2016, Article ID 4091732, 9 pages, 2016.
- [34] N. Zhang, C. Liu, and B. Chen, "A case study of presplitting blasting parameters of hard and massive roof based on the interaction between support and overlying strata," *Energies*, vol. 11, no. 6, pp. 1363–1377, 2018.
- [35] L. Ma, K. Li, X. Ding, H. Peng, and S. Xiao, "Development and application of blast casting technique in large-scale surface mines: a case study of Heidaigou surface coal mine in China," *Shock and Vibration*, vol. 2016, Article ID 8496742, 11 pages, 2016.

